ACS chemical biology

ACS AuthorChoice

Articles

pubs.acs.org/acschemicalbiology

Terms of Use

Substrate- and Cofactor-independent Inhibition of Histone Demethylase KDM4C

Ulrike Leurs,[†] Brian Lohse,*[,†] Kasper D. Rand,[‡] Shonoi Ming,[§] Erik S. Riise,[†] Philip A. Cole,[§] Jesper L. Kristensen,*[,†] and Rasmus P. Clausen*[,†]

[†]Department of Drug Design and Pharmacology, Faculty of Health and Medical Sciences, [‡]Department of Pharmacy, Faculty of Health and Medical Sciences, University of Copenhagen, Universitetsparken 2, DK-2100 Copenhagen, Denmark

[§]Department of Pharmacology and Molecular Sciences, Johns Hopkins University School of Medicine, 725 North Wolfe Street, 316 Hunterian Building, Baltimore, Maryland 21205, United States

Supporting Information

ABSTRACT: Inhibition of histone demethylases has within recent years advanced into a new strategy for treating cancer and other diseases. Targeting specific histone demethylases can be challenging, as the active sites of KDM1A-B and KDM4A-D histone demethylases are highly conserved. Most inhibitors developed up-to-date target either the cofactor- or substrate-binding sites of these enzymes, resulting in a lack of selectivity and off-target effects. This study describes the discovery of the first peptide-based inhibitors of KDM4 histone demethylases that do not share the histone peptide sequence or inhibit through substrate competition. Through screening of DNA-encoded peptide libraries against KDM1 and -4 histone demethylases by phage display, two cyclic peptides targeting the histone demethylase KDM4C were identified and developed as inhibitors by amino acid replacement, truncation, and chemical modifications. Hydrogen/deuterium exchange mass spectrometry revealed that the peptide-based inhibitors target KDM4C through substrate-independent interactions located on the surface remote from the active site within less conserved regions of KDM4C. The sites discovered in this study provide a new approach of targeting KDM4C through substrate- and cofactor-independent interactions and may be further explored to develop potent selective inhibitors and biological probes for the KDM4 family.

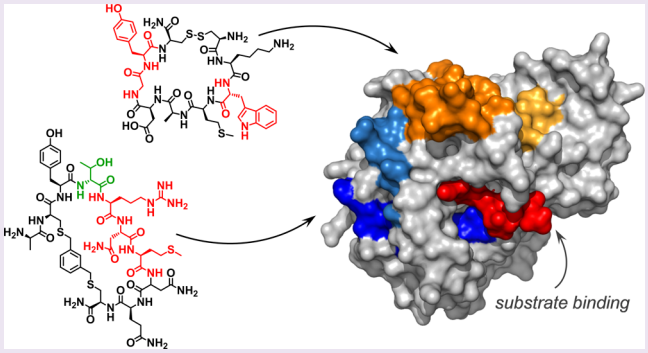

The dynamic regulation of gene expression is controlled by a range of mechanisms, among which reversible posttranslational modifications (PTM) of the N-terminal tails of histone proteins play an important role through affecting chromatin structure.[1,2] Deregulation of histone-modifying enzymes has been shown in a number of diseases, including cancer;[3] thus, inhibitors of histone-modifying enzymes are interesting probes for investigating the biological role of these enzymes and their potential as therapeutic targets.

Until the discovery of the histone demethylase KDM1A in 2004, histone methylation was thought to be an irreversible epigenetic mark.[4] KDM1A and its paralog KDM1B are FAD-dependent amino oxidases demethylating mono- and dimethylated lysine 4 on histone H3 (H3K4me2/me1). The KDM4 family of Jumonji-domain containing demethylases was identified in 2006[5] and consists of the six members KDM4A, -B, -C, -D, -E, and −F. Among those, KDM4E and -F are considered pseudo-genes,[6,7] while KDM4A-D produce enzymatically active gene products.[8] KDM4 demethylases are known to demethylate H3K9me2/3, H3K36me3/2, and H1.4K26me3/2 through a hydroxylation reaction requiring the cofactors Fe(II) and 2-oxoglutarate (2-OG).[5,9] Due to their elevated activity and expression in several forms of cancer, KDM1 and -4 proteins are recognized as oncogenes.[10,11] KDM1 is, among others, associated with prostate, bladder, and estrogen-receptor-negative breast cancer.[12] The KDM4 family of histone demethylases has repeatedly been shown to be involved in progression of hormone dependent cancers, such as breast and prostate cancer through coregulating hormone receptors.[13−15] The development of selective KDM1 or -4 inhibitors is impeded by the high structure and sequence conservation of these enzymes; most known inhibitors mimic either the FAD cofactor (KDM1) or 2-OG through Fe(II)-binding (KDM4) and hence interact with a plethora of other targets, such as 2-OG-dependent oxygenases through iron chelation.[16−19] The conjugation of iron chelating compounds to the truncated histone peptide substrate has been investigated as well,[20,21] and it resulted in the discovery of the first KDM4 selective inhibitors. However, there is a need for additional strategies to target histone demethylases through noncofactor and nonsubstrate interactions. Novel inhibitory

Received: May 14, 2014
Accepted: July 11, 2014
Published: July 11, 2014

scaffolds targeting alternative sites on histone demethylases are warranted, as they might hold the key to subfamily and isoform selectivity.

Herein, we present the discovery of several peptide binders of the histone demethylases KDM1A, -4A and -4C using phage display, which are not related to the sequence of their natural histone peptide substrates. Two of these peptides were developed into inhibitors of KDM4C by amino acid replacement, truncation, and chemical modifications. The inhibitors were found to target KDM4C via substrate-independent interactions on the surface of the enzyme located in neighboring regions of the highly conserved active site and within less conserved regions.

RESULTS AND DISCUSSION

Phage Display Screening. Phage display screening is a versatile tool for the discovery of peptides binding to biological targets such as proteins.[22] A phage library displaying random peptide sequences fused to the N-terminus of the phage protein pIII was screened against the catalytic domains of histone demethylases KDM1A, -1B, -4A, -4B, -4C, -4D, and -4E. The library consisted of linear 7- and 12-mer peptide sequences (X_7/X_{12}GGGS, X = random residues), and a cyclic peptide-phage library with two cysteines bridging a random 7-mer peptide sequence (ACX_7CGGGS). After 4−5 rounds of biopanning against the surface-immobilized target proteins, phages binding to KDM1 and -4 proteins were amplified in *E. coli*, and phage-ELISA revealed a number of potential KDM1 and -4 interacting peptides (PP1−6, Table 1). Both cyclic and linear peptides were identified, and the KDM1 and -4 binding phages did not share any sequence motifs. The apparent affinities of the phages were established to be in the low μM range from competition experiments performed between free and surface-immobilized KDM protein for phage binding (Table 1 and Supporting Information (SI) Figure S1). Cross affinity testing of peptide-phages PP1−6 against all KDM1 and -4 proteins revealed that most phages were specific binders (SI Table S2); however, PP5 displayed some affinity toward KDM1A, and PP3 showed weak affinity for several proteins.

Table 1. Peptide Sequences Targeting KDM1A, -B, and KDM4A−C Identified from Phage Display, As Well As the Apparent EC_{50} Values of the Peptide-Phages

protein	phage-peptide	sequence	EC_{50} [μM]
KDM1A	PP1	SHSEFWDWGPGGG	1.6
KDM1B	PP2	AWDVIWDQLLQH	10
KDM4A	PP3	GRMDWLGWRYELGGG	11
	PP4	SHSMSNRAPSALVRIGGG	3.4
KDM4C	PP5[a]	ACKWMDDGYCGGG	56
	PP6[a]	ACYTRNMNQCGGG	1.3

[a]Peptides cyclized via disulfide bridge on the phage surface.

After their identification from phage display, the inhibitory activity of the soluble peptides was assessed on their respective epigenetic target proteins. The peptides were initially synthesized including the phage-derived N- and C-terminal linker sequences, and C-terminally amidated to resemble the fusion to the phage protein pIII. The peptides were tested for demethylase inhibitory activity against their targets KDM1A, KDM1B, KDM4A, and KDM4C (SI Figures S2−6). The two cyclic peptides **1** (derived from PP5) and **2** (derived from PP6) inhibited KDM4C-mediated H3K9me3 demethylation with IC_{50} values of 1000 μM and 52 μM, respectively (Table 2).

Peptide Development. In order to increase the inhibitory activity of **1** and **2** which was dramatically decreased in comparison to the peptide-phages, their structures were optimized. It was hypothesized that weak inhibition of **1** in particular, but also **2**, might originate from instability of the peptides owing to the presence of aspartate and asparagine residues that are known to destabilize peptides in solution, leading to deamidation and isomerization.[23] Hence, the aspartate residues in peptide **1** were exchanged with alanine and/or glutamate, and the asparagine residues in **2** were exchanged with alanine. Single and double exchange of D6 and D7 to alanine in peptide **1** gave analogues **3**−**5**, and exchange to glutamate gave **6**−**8**. The exchange of D6A (**4**) led to a dramatic increase in inhibitory activity, and also the double substitution D6E/D7E resulted in an increase in inhibitory potency. These findings indicate that **1** might indeed be inactive due to stability issues. All other analogues of **1** were inactive. For **2**, exchanges N6A and N8A gave inactive peptides **9** and **10**, whereas the double exchange N6A/N8A yielded the 2-fold less active peptide **11**.

The initial synthesis of peptides **1** and **2** included the phage-derived linker sequences, an N-terminal alanine residue, and three C-terminal glycine residues. To reduce the size of the peptides, these nonrandomized sequences beyond the cysteines were removed sequentially. First, peptide **4** was truncated from either the N- or C-terminus, leading to inactive peptides **12** and **13**. Truncation from both ends (**14**) reduced inhibitory activity by only ∼10-fold. Truncation of **2** from the N- or both termini, leading to peptides **15** and **17**, resulted in loss of inhibitory activity, while truncation from the C-terminus (**16**) reduced inhibitory potency by ∼3-fold. Interestingly, also N-terminal acetylation of **2** (**24**) led to a complete loss of inhibitory activity on KDM4C, indicating that the N-terminal alanine residue serves an important function in inhibiting KDM4C.

Disulfide bridges in peptides can sometimes be unfavorable due to their tendency to undergo disulfide reshuffling in solution with other cysteine containing compounds,[24] such as the target protein KDM4C. An alternative to disulfide bridge cyclization is the coupling of cysteines using xylenes, which leads to a relatively small increase of the disulfide bond length and stabilizes it.[25] To investigate the effect of inserting xylenes into the disulfide bridge of **2**, the cysteines were linked by alkylation with *o*-, *m*- and *p*-α-α'-dibromoxylenes to give **18**, **19**, and **20** (Figure 1). Compounds **19** and **20** displayed comparable inhibitory activity to **2**, while **18** was inactive (SI Figure S7). *m*-Dibromoxylene insertion was pursued further by modifying the truncated peptides **16** and **14**, leading to analogues **21** and **22**, respectively. While the potency of **21** was increased ∼30-fold compared to **16**, peptide **22** was inactive.

To investigate the functionally important amino acids of **21** and **14** in more detail, two alanine scans were performed. The resulting 13 peptides were screened against KDM4C, and the average decrease in inhibitory activity was compared to the original peptides (Figure 2 and SI Figure S8). For **14**, all alanine analogues were less active than the original peptide (Figure 2A); however, the exchanges W3A, G7A, and Y8A led to the most profound decrease in activity, indicating that these residues form a conformational binding epitope for interaction with KDM4C. In case of **21**, KDM4C inhibition decreased with substitutions R5A, N6A, and M7A, suggesting a continuous linear binding sequence (Figure 2B). Interestingly, substitution T4A (**24**) led to

dx.doi.org/10.1021/cb500374f | *ACS Chem. Biol.* 2014, 9, 2131−2138

Table 2. Amino Acid Sequences of Peptides 1 and 2 and Their Analogues, IC_{50} Values, and Hill Slopes on KDM4C

peptide	sequence	IC_{50} [μM][a]	Hill slope
1	ACKWMDDGYCGGG[b]	1000	
2	ACYTRNMNQCGGG[b]	52 ± 1.5	−0.42
3	ACKWMAAGYCGGG[b]	>1000	
4	ACKWMADGYCGGG[b]	8.5 ± 1.5	−0.56
5	ACKWMDAGYCGGG[b]	>1000	
6	ACKWMEEGYCGGG[b]	~520	
7	ACKWMDEGYCGGG[b]	>1000	
8	ACKWMEDGYCGGG[b]	>1000	
9	ACYTRAMNQCGGG[b]	>1000	
10	ACYTRNMAQCGGG[b]	>1000	
11	ACYTRAMAQCGGG[b]	97 ± 1.5	−0.90
12	CKWMADGYCGGG[b]	>1000	
13	ACKWMADGYC[b]	>1000	
14	CKWMADGYC[b]	76 ± 1.3	−0.93
15	CYTRNMNQCGGG[b]	>1000	
16	ACYTRNMNQC[b]	406 ± 1.3	−0.55
17	CYTRNMNQC[b]	>1000	
21	Meta-Xyl-ACYTRNMNQC[c]	16 ± 1.6	−0.70
22	Meta-Xyl-CKWMADGYC[c]	>1000	
23	ACYTRNMNQCGGGYGRKKRRQRRR[b]	0.6 ± 0.02	−0.46
24	Ac-ACYTRNMNCGGG[b]	>1000	

[a]Determined by LANCEUltra KDM4C Histone H3K9 demethylase assay. K_m (ccKDM4C) = 220 nM, c ($H3K9me_3$) = 300 nM. Full dose−response curves are shown in SI Figure S6. [b]Peptides cyclized by disulfide bridge. [c]Peptides cyclized by *m*-α-α′-dibromoxylene.

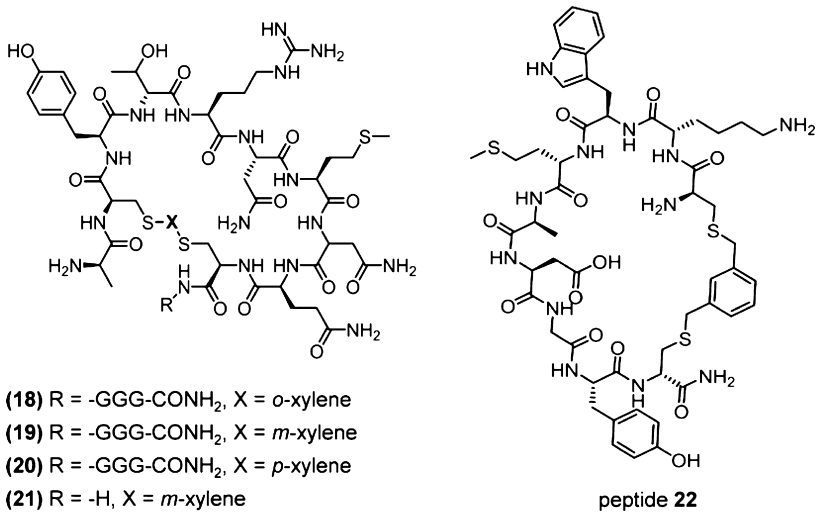

Figure 1. Compounds **18**−**22** cyclized by dibromoxylenes.

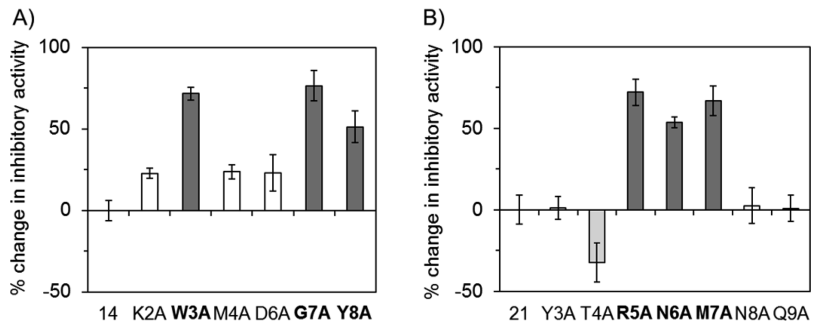

Figure 2. Average change in inhibitory activity of alanine analogues of peptide **14** (A) and **21** (B) on KDM4C normalized to the activity of the original peptides. Error bars are standard deviation of the mean (n = 3).

improved inhibition (IC_{50} = 2.6 μM), indicating that the more bulky threonine residue could hinder interaction with KDM4C.

Cellular Activity. The effects of compounds **2**, **4**, and **21** on cellular histone demethylation were investigated through cellular

dx.doi.org/10.1021/cb500374f | *ACS Chem. Biol.* 2014, 9, 2131−2138

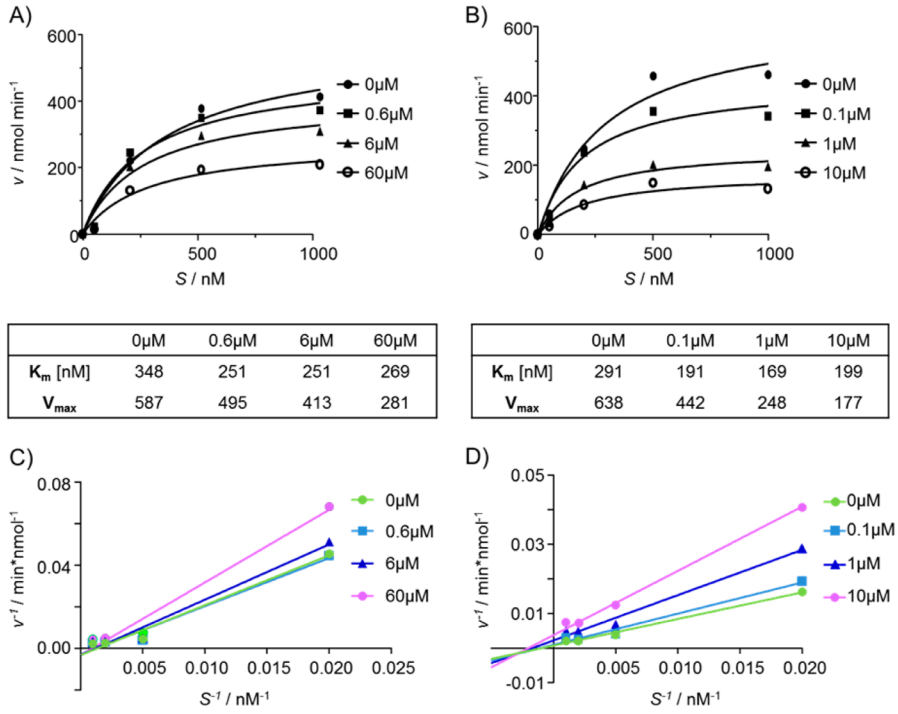

	0μM	0.6μM	6μM	60μM
K_m [nM]	348	251	251	269
V_{max}	587	495	413	281

	0μM	0.1μM	1μM	10μM
K_m [nM]	291	191	169	199
V_{max}	638	442	248	177

Figure 3. Substrate-dependent inhibition of KDM4C by **4** (A, C) and **23** (B, D). (A, B) The velocity of KDM4C at different inhibitor concentrations is plotted against the substrate concentration, the tables show the respective K_m and V_{max} values. (C, D) Corresponding Lineweaver−Burk plots.

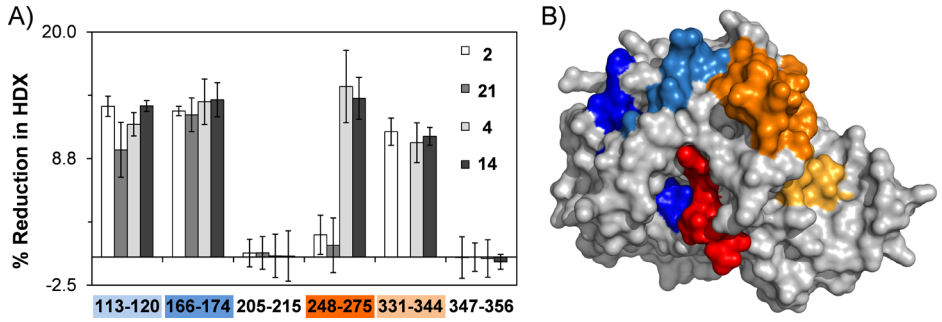

Figure 4. Differential HDX-MS data for KDM4C ± peptide inhibitors. (A) Histograms showing the percent reduction in HDX for KDM4C residues 113−120, 166−174, 205−215, 248−275, 331−344, and 347−356 by peptides **2**, **21**, **4**, and **14**. Values are calculated relative to the measured %D value for free KDM4C (n = 3, error bars are standard deviation of the mean). B) HDX data for the four regions of interest are plotted over the structure of KDM4C (pdb 2XML) with 113−120 highlighted in light blue, 166−174 in blue, 248−275 in orange, and 331−344 in light orange. The histone peptide substrate is shown in red.

immunofluorescence assays using osteosarcoma U2OS cells. In addition, the effect of attaching a cell penetrating TAT-peptide to the C-terminus of peptide **2** was investigated (peptide **23**). Though an increase in inhibitory activity was observed for **23** (Table 2), no cellular activity on histone demethylase activity could be detected for this or any of the other tested compounds (data not shown). Most likely, the lack of activity was due to low cell-permeability, cellular stability issues, and/or the insufficient inhibitory activity of the compounds.

Interaction with KDM4C. In order to investigate the mechanism by which the peptides inhibit KDM4C in more detail, the two best analogues from each series, **4** and **23**, were tested in substrate competition experiments. The Michaelis−Menten kinetics of KDM4C were determined at various inhibitor concentrations, as shown in Figure 3A, B. For both compounds, the K_m value initially decreased by ∼30% upon inhibitor addition but remained constant at higher inhibitor concentrations. In contrast to this behavior, the V_{max} values continuously decrease with increasing inhibitor concentration. These results imply that **4** and **23** do not simply inhibit KDM4C in a substrate-competitive manner, but through a type of noncompetitive inhibition. Also, the shift of the intersection in the Lineweaver−Burk plots to the right of the y-axis (Figure 3C, D) indicates an atypical mechanism of inhibition, potentially through cooperative binding with more than one peptide.

To dissect the mode of interaction between the inhibitors and KDM4C, hydrogen−deuterium exchange (HDX) mass spectrometry (MS) was employed to explore the sites affected by peptide-binding on KDM4C in solution. HDX-MS monitors the HDX of backbone amide hydrogens in a protein by MS;[26] HDX can be localized to different regions of the protein by pepsin proteolysis and mass analysis of the deuterium content of the resulting peptic peptides. A ligand binding event can cause a reduction in the deuterium uptake in regions of the protein involved in binding. Prior to HDX, the peptides were incubated with KDM4C for 30 min at room temperature (RT) to allow

dx.doi.org/10.1021/cb500374f | ACS Chem. Biol. 2014, 9, 2131−2138

binding of the peptide to the protein. Upon peptide addition, reductions in deuterium uptake were observed on KDM4C fragments 113−120 and 166−174 for peptides **2**, **4**, **14**, and **21** (Figure 4A and SI Figure S12). Peptides **4** and **14** showed additional alterations on 248−275, and **2**, **4**, and **14** on 331−344, suggesting distinct binding modes. Inspection of the interacting regions in the X-ray crystal structure of KDM4C indicates two regions affected by peptide binding; the first one spanning residues 113−120 (light blue) and 166−174 (blue) where all inhibitory peptides induce reduced deuterium uptake for KDM4C, and a second one covering 248−275 (orange) and 331−344 (light orange) on KDM4C (Figure 4B). All identified regions are located on the surface of KDM4C and remote from the substrate binding site (red). To verify that no interaction takes place in the active site, regions involved in substrate binding (205−215) and catalytic activity (347−356)[27] were analyzed as well, but no changes in HDX upon peptide addition could be detected (Figure 4A). Thus, inhibition seems to occur through interactions on the surface of KDM4C. The identified sites are located within less conserved regions remote from the active site of KDM4C, suggesting a potential selectivity toward inhibition of distinct isoforms of the KDM4 family. These sites are also remote from the N- and C-terminal tails of the construct and are most likely accessible on the full-length enzyme, since the rest of the protein sequence of the enzyme continues on the back side of the view in Figure 4B. However, it remains to be established that the compounds can inhibit full length enzymes. Considering that the two surfaces (spanning from 113 to 120 and 166−174, and 248−275 and 331−344) are too far apart to be reached by a single peptide molecule, these results support the previously hypothesized cooperative binding of the peptides to KDM4C. Furthermore, the overall negative Hill slopes of the inhibitors (Table 2) also indicate negative cooperative binding of the inhibitors to KDM4C. Interestingly, it has been suggested in the literature that the interactions between phage-display-derived peptides and their target proteins are not only driven by the monomeric sequence of the peptide but by its multimeric presentation on the phage.[28] The shown results could be interpreted to support this suggestion.

Both the cross affinity screening on phage-level (SI Table S2) and the results from the HDX-MS analysis indicate that the peptides could display a certain level of isoform selectivity. The cross affinity screening showed that PP5 (developed into **4**) has the highest affinity on KDM4A, while PP6 (developed into **2** and **21**) binds primarily to KDM4C. To test the peptides' isoform selectivity, **2**, **4**, and **21** were tested for their inhibitory activity on KDM4A and -B by AlphaScreen, revealing that all three peptides inhibit KDM4A and -B to various degrees, with **21** being the most potent inhibitor, and **2** and **4** showing overall lower activity (SI Figure S9). For all tested compounds, KDM4A shows the highest level of inhibition, followed by KDM4C and then KDM4B. These results are in good agreement with the degree of structural conservation among KDM4A-C, which is highest between KDM4A and -C. The IC_{50} values of **21** on KDM4A, -B, and -C were determined in separate dose−response experiments from AlphaScreen and ranged from 1.1 μM for KDM4B to 2.1 μM for KDM4A and 3.5 μM for KDM4C (SI Figure S10). These results show that there is no selectivity of the compounds among the KDM4 family. In principle, the compounds could also have activity at other demethylases, but it is the aim of future studies to establish a complete selectivity profile.

Conclusion. In conclusion, phage display screening provided a viable platform to identify inhibitors of histone demethylases. Though the initial hits discovered by phage display showed only moderate inhibitory behavior, it was possible to develop them into more potent compounds through amino acid replacement, truncation, and chemical modifications. The optimized KDM4C inhibitors were analyzed biochemically with respect to their target engagement, suggesting that inhibition takes place through a mechanism that is not competitive and potentially involves cooperative binding. This hypothesis was further supported by the HDX-MS analysis that suggested two distinct binding surfaces on the catalytic core of KDM4C located remote from the active site. Initial optimization of the peptides increased the potency of the inhibitors but did not lead to isoform selectivity. However, since the sites affected by peptide binding were found to be located within a less conserved region of KDM4C, and the phage display also suggested isoform selectivity, the peptide sequences described may be developed into selective inhibitors for individual KDM4 isoforms. It can further be speculated that the peptides target protein−protein interactions, or dimerization sites of KDM4C. Multiprotein complexes containing KDM4C are believed to be important for the recruitment of the demethylase to transcription sites; hence, the peptides could potentially be used as tool compounds to abolish such interactions. The dimerization of KDM4C has been demonstrated in the literature;[29] however, it remains unknown whether the enzyme is functional as a mono- or as a dimer. Also, the dimerization interface of KDM4C is unknown, albeit all KDM4 proteins normally crystallize as dimers. Though this dimerization might be artifically induced through the high protein concentrations required for crystal formation, the crystal structure of KDM4C (pdb 2XML) indicates that the dimerization surface is located between the N-terminal JmjN domain and the β-hairpin (residues 112−135). If this site is involved in dimer formation and dimerization is crucial for demethylase activity, the binding of the peptides to this site, as shown by HDX-MS, would disrupt the dimer and inhibit the enzyme. Additional studies are, however, needed to verify this. Based on our findings, we believe that the herein described compounds are important new lead structures for developing potent, selective tool compounds for both epigenetic therapy and the study of the physiological role of KDM4C. Future studies will aim at increasing potency through developing these interesting scaffolds by further modifications and to further characterize the biological activity of these peptides. Moreover, important goals will be to induce isoform selectivity and cell-activity of the peptides.

METHODS

Phage Display. Two linear 7-mer and 12-mer and a constrained version of the peptide library were used for the selection. Microtiter plates were coated at 4 °C for 16 h with 10 μM purified protein in 1× PBS (20 mM sodium phosphate, 150 mM NaCl, pH 7.4, total volume per well 100 μL). The microtiter plates were subsequently washed with 1× PBS and then blocked with 4% skim milk in 1× PBS for 1 h at RT. Bacteriophages at around 10^{10}−10^{11} pfu/ml were used for each panning round. The constrained and linear libraries were mixed and panned together in 1× PBS. After incubation for 1 h at RT, the plates were washed 10 times with 1× PBS and bound peptide-phages were eluted with glycine/HCl, pH = 2.2 for 10 min, followed by neutralization with Tris-base, pH = 9.0. Eluted phages were used to infect exponentially growing TG1 cells overnight at 37 °C. The following day, the peptide phages were precipitated from the cell supernatant with phage precipitation buffer (20% (w/v) PEG6000 in 2.5 M NaCl) and redissolved in 300 μL 1× PBS. After 4−5 rounds of panning, single clones were isolated and tested for KDM4A−E and KDM1A and -B

dx.doi.org/10.1021/cb500374f | ACS Chem. Biol. 2014, 9, 2131−2138

binding in phage ELISA (procedure described in the Supporting Information). Single stranded DNA was extracted from positive clones,[30] and the DNA was sequenced in the region corresponding to the random peptide region.

More experimental details and the protocols for phage and peptide ELISA are shown in the Supporting Information.

LANCE Ultra KDM4C Histone H3-Lysine 9 Demethylase Assay. For inhibition studies on KDM4C, PerkinElmer's LANCE Ultra JMJD2C Histone H3-Lysine 9 demethylase assay was performed according to the manufacturer's protocol. The catalytic core domain of KDM4C (ccKDM4C) employed in the LANCE assay was prepared as described previously.[21] Assays were carried out in triplicate measurements at RT; the total reaction volume was 10 μL/well. For inhibition studies, 0.6 fmol ccKDM4C were incubated for 30 min with various concentrations of the peptides prior to addition of the substrate mix, containing 300 nM H3K9me3 peptide substrate. The reaction mixture was allowed to incubate for another 30 min at RT, before the reaction was stopped by addition of the detection mix. The TR-FRET signal was read using a Safire2TM microplate reader (Tecan). Reaction mixtures of assay buffer without enzyme or without inhibitor were used as controls. For curve fitting and data analysis, GraphPad Prism 6.0 was used. All experiments were performed at least in triplicate.

FDH-Coupled KDM4A Activity Assay. The FDH-coupled KDM4A activity assay was performed according to a protocol described by Leurs et al.[31] Instead of 0.015 mg ccKDM4C, an equimolar amount of ccKDM4A was used.

AlphaScreen KDM4A, -B, and -C Demethylase Assay. All of the enzymatic reactions were conducted in duplicate at RT for 60 min in a 10 μL mixture containing assay buffer, histone H3 peptide substrate, demethylase enzyme, and the test compound. These 10 μL reactions were carried out in wells of 384-well Optiplate (PerkinElmer). After enzymatic reactions, 5 μL of anti-Mouse Acceptor beads (PerkinElmer, diluted 1:250 with 1× detection buffer and 5 μL of primary antibody (BPS, diluted 1:100 with 1× detection buffer) were added to the reaction mix. After brief shaking, the plate was incubated for 30 min. Finally, 10 μL of AlphaScreen Streptavidin-conjugated donor beads (PerkinElmer, diluted 1:125 with 1× detection buffer) were added. In 15 min, the samples were measured in AlphaScreen microplate reader (EnSpire Alpha 2390 Multilabel Reader, PerkinElmer). Enzyme activity assays were performed in duplicates at each concentration. The AlphaScreen intensity data were analyzed and compared. In the absence of the compound, the intensity (C_e) in each data set was defined as 100% activity. In the absence of enzyme, the intensity (C_0) in each data set was defined as 0% activity. The percent activity in the presence of each compound was calculated according to the following equation: % activity = $(C - C_0)/(C_e - C_0)$, where C is the A-screen intensity in the presence of the compound.

KDM1A and -B Demethylase Assay. For inhibition studies on KDM1A and -B, a peroxidase-coupled assay monitoring hydrogen peroxide production was performed as previously described.[32] KDM1A was purchased from BPSBioscience (Cat. No. 50097); KDM1B cloning, expression, and purification.[33] The time courses of the reaction were measured under aerobic conditions using a Beckman Instruments DU series 600 spectrophotometer equipped with a thermostat-controlled cell holder (T = 25 °C). The 100 μL reactions were initiated by addition of enzyme (100−200 nM KDM1A, or 480 nM KDM1B) to reaction mixtures consisting of 50 mM HEPES buffer (pH 7.5), 0.1 mM 4-aminoantipyrine, 1 mM 3,5-dichloro-2-hydroxybenzene-sulfonic acid, 0.76 μM horseradish peroxidase (Worthington Biochemical Corp.), 100 μM inhibitor, and 24 μM or 100 μM H3K4me2 for KDM1A and KDM1B, respectively. Absorbance changes were monitored at 515 nm, and an extinction coefficient of 26 000 M^{-1} cm^{-1} was used to calculate product formation. For curve fitting and data analysis, GraphPad Prism 6.0 was used.

Cellular Immunofluorescence Assay. U2OS cells were seeded 24 h before transfection. Transfection was performed with Fugene HD transfection reagent as recommended by the manufacturer. Six hours after transfection, the cells were harvested and seeded into multi-well plates into media containing compound. Twenty hours after incubation of cells with compounds, the cells were washed once in PBS, harvested by fixation with formaldehyde 4% aqueous solution, and washed 2 times in PBS. Subsequently, the cells were permeabilised in PBS, 0.2% Triton X-100 for 10 min at RT. Blocking was performed in PBS, 0.2% Triton X-100, 5% FBS for 45 min at RT. The cells were incubated with primary antibodies diluted 1 μg mL^{-1} in blocking solution overnight at 4 °C. The primary antibodies used in the assays were HA.11 (Covance, MMS-101P) and the antibodies detecting the marks are specified in SI Table S3. After incubation with primary antibodies, the cells were washed 3 times with PBS, incubated with secondary antibodies diluted 1:1000 (Alexa fluor 594 goat anti rabbit IgG, Invitrogen, A11012; Alexa flour 488 donkey anti-mouse IgG, Invitrogen, A21202) and Hoechst, 20 μg mL^{-1} (Sigma, 33342) in blocking solution, and washed again 3 times with PBS. Finally, PBS was added and high throughput imaging and analysis were performed by an IN Cell Analyzer 1000 (GE Healthcare). In the analysis, individual cells were divided into HA^+ (transfected cells) and HA^- (nontransfected cells). The IC_{50} values were based on an average measure of the staining of the mark specified in SI Table S3 in the transfected cells.

Hydrogen/Deuterium Exchange Mass Spectrometry (HDX-MS). The peptides were preincubated with ccKDM4C (expressed and purified as for LANCE inhibition testing) for 30 min in order to allow target binding equilibration prior to deuterium labeling. Continuous amide H/D exchange was initiated by a 10-fold dilution of protiated protein solutions in the presence or absence of peptide into the corresponding deuterated buffer (12.5 mM HEPES pH 7.4, 5 μM $FeSO_4$, 100 μM ascorbate). Nondeuterated controls were prepared by dilution into an identical protiated buffer. All HDX reactions were carried out at RT and contained 1.2 μM ccKDM4C in the absence or presence of 160 μM peptide. At appropriate time points ranging from 15 s to 4 h, aliquots of the HDX reaction were quenched by addition of an equal volume of ice-cold quenching buffer (300 mM phosphate (pH 2.3) and 50 mM TCEP) resulting in a final pH of 2.5. Quenched samples were immediately frozen and stored at −80 °C. Samples were injected into a cooled Waters nanoAcquity UPLC system for online pepsin digestion and rapid desalting of the protein samples. After digestion of the samples, the peptic peptides were trapped on a trap column (Waters VanGuard C18, 1.7 μm, 2.1 × 5 mm) and desalted with 0.68% formic acid in 8% acetonitrile, pH 2.3, 200 μL min^{-1} for 3 min. Peptides were eluted from the trap to the analytical column (Waters XBridge C_{18}, 1.7 μm, 1.0 × 100 mm) and separated with an 8−40% gradient of 0.68% formic acid in acetonitrile (pH 2.3) over 12 min at a flow rate of 40 μL/min. Positive ion-electrospray ionization mass spectra of eluted peptides were acquired on a Waters SynaptG2 HDMS mass spectrometer. Peptic peptides were identified in separate experiments using collision-induced dissociation tandem mass spectrometry performed with a data-independent (MS^E) acquisition scheme. A sequence coverage map of peptic peptides of KDM4C identified from this analysis is shown in SI Figure S11. The sequence coverage was 91.7% with a redundancy of 1.84. Mass spectra were processed using the MassLynx and DynamX software packages (Waters Corp.). Complete deuteration of control samples was achieved by incubation of 60 pmol KDM4C in the deuterated buffer in the presence of 6 M guanidine for 24 h at 30 °C. Average back exchange (i.e., deuterium loss) was measured as 37% for the analyzed peptides. However, no corrections were made for this deuterium loss as only the relative levels of deuterium incorporation of all samples were compared. The HDX of KDM4C in the presence and absence of peptide after 10 min exchange was measured in triplicate to confirm the significance of the detected changes in deuterium uptake, Significant changes were defined as 3× SD. HDX-MS analysis of KDM4C was also performed in the presence of the nonbinding Peptide 1 and no significant changes in HDX was observed in KDM4C due to the presence of Peptide 1 (data not shown). For peptide 21, KDM4C fragment 331−344 showed complex bimodal HDX kinetics that require further investigation (data not shown). Protein structures were visualized using PyMOL (DeLano Scientific).

■ ASSOCIATED CONTENT

Supporting Information

Additional methods, figures, and tables. This material is available free of charge via the Internet at http://pubs.acs.org.

■ AUTHOR INFORMATION

Corresponding Authors

*Email: rac@sund.ku.dk.
*Email: jesper.kristensen@sund.ku.dk.
*Email: bril@sund.ku.dk.

Notes

The authors declare no competing financial interest.

■ ACKNOWLEDGMENTS

The Danish Cancer Society and University of Copenhagen Programme of Excellence are gratefully acknowledged. K.D.R. acknowledges support from the Marie Curie Actions Programme of the E.U. (Grant No. PCIG09-GA-2011-294214) and the Danish Council for Independent Research|Natural Sciences (Steno Grant No. 11-104058). We thank the National Institutes of Health (NIH) for support (P.A.C., S.M.). We thank D. V. Larsen and H. R. Hudlebusch from EpiTherapeutics ApS for performing the immunofluorescence measurements.

■ REFERENCES

(1) Van Holde, K. E. (1988) *Chromatin*; Springer-Verlag, New York.
(2) Bojang, P., Jr., and Ramos, K. S. (2014) The promise and failures of epigenetic therapies for cancer treatment. *Cancer Treat Rev. 40*, 153−169.
(3) Plass, C., Pfister, S. M., Lindroth, A. M., Bogatyrova, O., Claus, R., and Lichter, P. (2013) Mutations in regulators of the epigenome and their connections to global chromatin patterns in cancer. *Nat. Rev. Genet. 14*, 765−780.
(4) Shi, Y., Lan, F., Matson, C., Mulligan, P., Whetstine, J. R., Cole, P. A., and Casero, R. A. (2004) Histone demethylation mediated by the nuclear amine oxidase homolog LSD1. *Cell 119*, 941−953.
(5) Cloos, P. A., Christensen, J., Agger, K., Maiolica, A., Rappsilber, J., Antal, T., Hansen, K. H., and Helin, K. (2006) The putative oncogene GASC1 demethylates tri- and dimethylated lysine 9 on histone H3. *Nature 442*, 307−311.
(6) Katoh, M., and Katoh, M. (2004) Identification and characterization of JMJD2 family genes in silico. *Int. J. Oncol. 24*, 1623−1628.
(7) Whetstine, J. R., Nottke, A., Lan, F., Huarte, M., Smolikov, S., Chen, Z., Spooner, E., Li, E., Zhang, G., Colaiacovo, M., and Shi, Y. (2006) Reversal of histone lysine trimethylation by the JMJD2 family of histone demethylases. *Cell 125*, 467−481.
(8) Berry, W. L., and Janknecht, R. (2013) KDM4/JMJD2 histone demethylases: Epigenetic regulators in cancer cells. *Cancer Res. 73*, 2936−2942.
(9) Trojer, P., Zhang, J., Yonezawa, M., Schmidt, A., Zheng, H., Jenuwein, T., and Reinberg, D. (2009) Dynamic histone H1 isotype 4 methylation and demethylation by histone lysine methyltransferase G9a/KMT1C and the Jumonji domain-containing JMJD2/KDM4 proteins. *J. Biol. Chem. 284*, 8395−8405.
(10) Liu, G., Bollig-Fischer, A., Kreike, B., van de Vijver, M. J., Abrams, J., Ethier, S. P., and Yang, Z. Q. (2009) Genomic amplification and oncogenic properties of the GASC1 histone demethylase gene in breast cancer. *Oncogene 28*, 4491−4500.
(11) Amente, S., Lania, L., and Majello, B. (2013) The histone LSD1 demethylase in stemness and cancer transcription programs. *Biochim. Biophys. Acta 1829*, 981−986.
(12) Kooistra, S. M., and Helin, K. (2012) Molecular mechanisms and potential functions of histone demethylases. *Nat. Rev. Mol. Cell Biol. 13*, 297−311.
(13) Wissmann, M., Yin, N., Muller, J. M., Greschik, H., Fodor, B. D., Jenuwein, T., Vogler, C., Schneider, R., Gunther, T., Buettner, R., Metzger, E., and Schule, R. (2007) Cooperative demethylation by JMJD2C and LSD1 promotes androgen receptor-dependent gene expression. *Nat. Cell Biol. 9*, 347−353.
(14) Shin, S., and Janknecht, R. (2007) Activation of androgen receptor by histone demethylases JMJD2A and JMJD2D. *Biochem. Biophys. Res. Commun. 359*, 742−746.
(15) Suikki, H. E., Kujala, P. M., Tammela, T. L., van Weerden, W. M., Vessella, R. L., and Visakorpi, T. (2010) Genetic alterations and changes in expression of histone demethylases in prostate cancer. *Prostate 70*, 889−898.
(16) Miller, M. J. (1989) Syntheses and therapeutic potential of hydroxamic acid based siderophores and analogs. *Chem. Rev. 89*, 1563−1579.
(17) Woon, E. C., Tumber, A., Kawamura, A., Hillringhaus, L., Ge, W., Rose, N. R., Ma, J. H., Chan, M. C., Walport, L. J., Che, K. H., Ng, S. S., Marsden, B. D., Oppermann, U., McDonough, M. A., and Schofield, C. J. (2012) Linking of 2-oxoglutarate and substrate binding sites enables potent and highly selective inhibition of JmjC histone demethylases. *Angew. Chem., Int. Ed. Engl. 51*, 1631−1634.
(18) Hojfeldt, J. W., Agger, K., and Helin, K. (2013) Histone lysine demethylases as targets for anticancer therapy. *Nat. Rev. Drug Discovery 12*, 917−930.
(19) Suzuki, T., and Miyata, N. (2011) Lysine demethylases inhibitors. *J. Med. Chem. 54*, 8236−8250.
(20) Lohse, B., Kristensen, J. L., Kristensen, L. H., Agger, K., Helin, K., Gajhede, M., and Clausen, R. P. (2011) Inhibitors of histone demethylases. *Bioorg. Med. Chem. 19*, 3625−3636.
(21) Lohse, B., Nielsen, A. L., Kristensen, J. B., Helgstrand, C., Cloos, P. A., Olsen, L., Gajhede, M., Clausen, R. P., and Kristensen, J. L. (2011) Targeting histone lysine demethylases by truncating the histone 3 tail to obtain selective substrate-based inhibitors. *Angew. Chem., Int. Ed. Engl. 50*, 9100−9103.
(22) Smith, G. P. (1985) Filamentous fusion phage: Novel expression vectors that display cloned antigens on the virion surface. *Science 228*, 1315−1317.
(23) Geiger, T., and Clarke, S. (1987) Deamidation, isomerization, and racemization at asparaginyl and aspartyl residues in peptides. Succinimide-linked reactions that contribute to protein degradation. *J. Biol. Chem. 262*, 785−794.
(24) Jaenicke, R. (1991) Protein stability and protein folding. *Ciba Found. Symp. 161*, 206−216 discussion 217−221.
(25) Timmerman, P., Beld, J., Puijk, W. C., and Meloen, R. H. (2005) Rapid and quantitative cyclization of multiple peptide loops onto synthetic scaffolds for structural mimicry of protein surfaces. *ChemBioChem 6*, 821−824.
(26) Hoofnagle, A. N., Resing, K. A., and Ahn, N. G. (2003) Protein analysis by hydrogen exchange mass spectrometry. *Annu. Rev. Biophys. Biomol. Struct. 32*, 1−25.
(27) Hillringhaus, L., Yue, W. W., Rose, N. R., Ng, S. S., Gileadi, C., Loenarz, C., Bello, S. H., Bray, J. E., Schofield, C. J., and Oppermann, U. (2011) Structural and evolutionary basis for the dual substrate selectivity of human KDM4 histone demethylase family. *J. Biol. Chem. 286*, 41616−41625.
(28) Gray, B. P., Li, S., and Brown, K. C. (2013) From phage display to nanoparticle delivery: Functionalizing liposomes with multivalent peptides improves targeting to a cancer biomarker. *Bioconjugate Chem. 24*, 85−96.
(29) Shin, S., and Janknecht, R. (2007) Diversity within the JMJD2 histone demethylase family. *Biochem. Biophys. Res. Commun. 353*, 973−977.
(30) Sambrook, J., Fritsch, E. F., and Maniatis, T. (1989) *Molecular cloning*, 2nd ed., Cold Spring Harbor Laboratory Press, Cold Spring Harbor, NY.
(31) Leurs, U., Clausen, R. P., Kristensen, J. L., and Lohse, B. (2012) Inhibitor scaffold for the histone lysine demethylase KDM4C (JMJD2C). *Bioorg. Med. Chem. Lett. 22*, 5811−5813.
(32) Forneris, F., Binda, C., Vanoni, M. A., Battaglioli, E., and Mattevi, A. (2005) Human histone demethylase LSD1 reads the histone code. *J. Biol. Chem. 280*, 41360−41365.

(33) Prusevich, P., Kalin, J. H., Ming, S. A., Basso, M., Givens, J., Li, X., Hu, J., Taylor, M. S., Cieniewicz, A. M., Hsiao, P.-Y., Huang, R., Roberson, H., Adejola, N., Avery, L. B., Casero, R. A., Taverna, S. D., Qian, J., Tackett, A. J., Ratan, R. R., McDonald, O. G., Feinberg, A. P., and Cole, P. A. (2014) A selective phenelzine analogue inhibitor of histone demethylase LSD1. *ACS Chem. Biol.*, DOI: 10.1021/cb500018s.